RADC-TR-76-403
Interim Technical Report
October 21, 1976

EVALUATION OF SULFOSALTS

Westinghouse Research Laboratories

Sponsored by Defense Advanced Research
Projects Agency (DoD) ARPA Order No. 3151

ROME AIR DEVELOPMENT CENTER
AIR FORCE SYSTEMS COMMAND
GRIFFISS AIR FORCE BASE, NEW YORK 13441

ARPA Order Number

3151

Program Code Number

6D10

Name of Contractor

Westinghouse Research Labs

Effective Date of Contract

April 15, 1976

Contract Number

F19628-76-C-0158

Principal Investigator and Phone Number

Thelma J. Isaacs
(412) 256-3557

RADC Project Scientist and Phone Number (617) 861-2211

Dr. Stanley K. Dickinson

Contract Expiration Date

October 15, 1977

This report has been reviewed by the RADC Information Office (OI) and is releasable to the National Technical Information Service (NTIS). At NTIS it will be releasable to the general public, including foreign nations.

Stanley K. Dickinson

STANLEY K. DICKINSON
Contract Monitor
Solid State Sciences Division

UNCLASSIFIED

SECURITY CLASSIFICATION OF THIS PAGE (When Data Entered)

REPORT DOCUMENTATION PAGE

READ INSTRUCTIONS BEFORE COMPLETING FORM

1. REPORT NUMBER: RADC-TR-76-403	2. GOVT ACCESSION NO.
3. RECIPIENT'S CATALOG NUMBER	
4. TITLE (and Subtitle): EVALUATION OF SULFOSALTS.	5. TYPE OF REPORT & PERIOD COVERED: First Semi-Annual Report No. 1
6. PERFORMING ORG. REPORT NUMBER: 76-9C4-SASSI-R1	
7. AUTHOR(s): T. J. Isaacs, R. W. Weinert, and J. P. McHugh	8. CONTRACT OR GRANT NUMBER(s): F19628-76-C-0158, ARPA Order-3151
9. PERFORMING ORGANIZATION NAME AND ADDRESS: Westinghouse Research Laboratories, 1310 Beulah Road, Pittsburgh, PA 15235	10. PROGRAM ELEMENT, PROJECT, TASK AREA & WORK UNIT NUMBERS: 61101E, P 3151 WU # 3151ARAA, ARPA Order No. 3151
11. CONTROLLING OFFICE NAME AND ADDRESS: Advanced Research Projects Agency, 1400 Wilson Boulevard, Arlington, VA 22209	12. REPORT DATE: December 1976
	13. NUMBER OF PAGES: 33
14. MONITORING AGENCY NAME & ADDRESS (if different from Controlling Office): Deputy for Electronic Technology (RADC), Hanscom AFB, Massachusetts 01731, Monitor/Stanley Dickinson/ETSP	15. SECURITY CLASS. (of this report): UNCLASSIFIED
	15a. DECLASSIFICATION/DOWNGRADING SCHEDULE

16. DISTRIBUTION STATEMENT (of this Report)

Approved for public release; distribution unlimited.

Semi-annual rept. no. 1

17. DISTRIBUTION STATEMENT (of the abstract entered in Block 20, if different from Report)

18. SUPPLEMENTARY NOTES

19. KEY WORDS (Continue on reverse side if necessary and identify by block number)

zero temperature coefficient of delay directions
thallium vanadium sulphide
crystal growth
furnace and control system
optimum composition
surface-wave filter
dielectric constant
bulk-wave resonator
piezoelectric constant

20. ABSTRACT (Continue on reverse side if necessary and identify by block number)

Investigations into phase equilibria relations in the system Tl-V-S show it to be complex, with multiple arrests and supercooling presenting problems in determining composition and melting relationships. The maximum melting composition has not as yet been determined, but it probably does not lie on any "pseudobinary" join. The best crystals which we have grown have been of nonstoichiometric composition, fractionally richer in Tl and S_2.

DD FORM 1 JAN 73 1473 EDITION OF 1 NOV 65 IS OBSOLETE

376 670

UNCLASSIFIED

SECURITY CLASSIFICATION OF THIS PAGE (When Data Entered)

20.

Studies on parameters of crystal growth are proceeding, with work now being performed varying the rate of growth while keeping the composition constant.

The material constants and their temperature coefficients have been measured and, with the exception of the piezoelectric constant temperature coefficient, ~~we expect~~ little change in these constants as crystal quality improves. The computer program used to calculate surface wave properties is being re-worked and should be available for use shortly. A SAW filter has been demonstrated on the (001) plane of Tl_3VS_4.

X is expected

TABLE OF CONTENTS

LIST OF ILLUSTRATIONS

LIST OF TABLES

EVALUATION OF SULFOSALTS

Semi-Annual Report
Contract No. F19628-76-C-0158

1. INTRODUCTION

1.1 Program Objectives

This program has two principal objectives, one of which is to determine the optimum conditions for fabrication of reproducible, high-quality crystals of Tl_3VS_4 and, if time permits, of related materials. The other is to determine directions in these crystals which have zero temperature coefficients of delay (ZTCD) for surface acoustic waves, and to assess which of these directions possesses the best combination of velocity, k^2, and power flow angle for device applications. New determinations of physical parameters (attenuation, velocities, k^2) will be made on improved crystals.

In addition, the effects of wider temperature ranges and higher order temperature coefficients of velocity will be examined. Hall measurements also will be made. A bandpass filter will be fabricated to demonstrate the applicability of these materials for surface-wave devices.

1.2 General Approach

The determination of the optimum composition for crystal growth is being done by studying phase relations around the composition Tl_3VS_4 in the ternary system Tl-V-S. The methods employed include thermal heating and cooling curves and quenching experiments. Further compositional refinement will then be accomplished by a series of crystal growth runs on samples having incremental differences in composition.

The search for ZTCD directions, in addition to the ones already known, is being done initially by use of a computer program which can theoretically find these directions, given a selected set of parameters. The information thus acquired will be tested experimentally on crystals, and the direction for optimum performance ascertained.

1.3 Summary

Investigations into phase equilibria relations in the system Tl-V-S show it to be complex, with multiple arrests and supercooling presenting problems in determining composition and melting relationships. The maximum melting composition has not as yet been determined, but it probably does not lie on any "pseudobinary" join. The best crystals which we have grown have been of nonstoichiometric composition, fractionally richer in Tl and S_2.

Studies on parameters of crystal growth are proceeding, with work now being performed varying the rate of growth while keeping the composition constant.

The material constants and their temperature coefficients have been measured and, with the exception of the piezoelectric constant temperature coefficient, we expect little change in these constants as crystal quality improves. The computer program used to calculate surface wave properties is being re-worked and should be available for use shortly. A SAW filter has been demonstrated on the (001) plane of Tl_3VS_4.

2. TECHNIQUES OF MATERIALS PREPARATION, PHASE EQUILIBRIA STUDIES, AND CRYSTAL GROWTH

2.1 Techniques of Materials Preparation

The reactant materials used for phase equilibria studies and for crystal growth are prepared from the high-purity elements (> 99.999 wt.% purity) Tl, V, and S. As Tl and V tend to oxidize readily, considerable care is taken to ensure that the surfaces of these elements are entirely free from oxide contamination. The oxide coating the Tl is removed by first heating the ingot in deionized water, followed by ultrasonic agitation and a final rinse in deionized water. The beaker of water containing the cleaned ingot is placed into a glove bag under nitrogen atmosphere. The ingot is removed from the water and blown dry using "Dust-Off". It is then set into an ampoule which is placed on the vacuum system, and the ampoule alternately evacuated and backfilled with argon a number of times, and then left under high vacuum for approximately 30 minutes to ensure thorough drying. The Tl is placed in a pre-weighed bottle in the N_2-filled glove bag, the tightly-fitting stopper inserted into the bottle, and weighed outside the glove bag. The container and its contents are then returned to the glove bag, and the ingot then placed into a silica-glass tube which is immediately evacuated.

The oxide coating the V is removed by use of a weak nitric acid bath. This is followed by thorough washing with deionized water. It is dried in a glove bag under N_2, and weighed quickly in air. The V is then returned immediately to the glove bag.

Sulphur requires no special handling, and is weighed in air and then placed into the silica-glass tubes via the N_2-filled glove bag.

The tubes containing these three elements are sealed under a pressure of $<5 \times 10^{-6}$ torr, and placed in horizontal split furnaces which have been preheated to between 500-700°C to encourage rapid reaction and lessen the possibility of explosion. After reaction occurs the temperatures are raised to between 700° and 750°C. The ampoules containing the molten material are held at these temperatures for 7 days, with intermittant vigorous shaking to promote homogeneity. When the reactant material is to be used for crystal growing or for determination of heating and cooling curves, it is cooled slowly to room temperature. When it is to be used for quench-type studies, it is quickly chilled in an ice water bath.

2.2 Techniques of Phase Diagram Study

Two techniques are being used for the phase diagram study, thermal analysis and quench-type (or silica-tube) experiments. Both types of experiments are being conducted in sealed, initially evacuated, silica-glass containers, which are well-suited for reactions among chalcogenide compounds of low or moderate melting points because they are inert, and because they constitute sealed containers for volatile components such as sulphur.

The same high-purity materials are being used in this part of the work as are described in Section 2.1, and the methods of cleaning the surfaces of Tl and V are identical with those described in that section.

The experimental system for thermal analysis consists of a well-lagged furnace, a temperature control system, and a strip chart recorder which produces a direct plot of sample temperature as a function of time. The sample material is contained in silica-glass ampoules containing a well into which a chromel-alumel thermocouple is inserted. The thermocouple is tied to the ampoule with nichrome wire, and then it is passed out of the furnace through a narrow opening. The ampoule

itself is seated vertically in a ceramic block. The thermocouple cold junction is placed in an ice bath. Most of the data are being collected from cooling curves, but as there is considerable supercooling, we also are obtaining information from heating curves. The rates of cooling which we have been using vary from as fast as 1°C/min to a much slower speed of 10°C/hour. Most of the experiments are being run at the slower rates as the problem of supercooling is then less severe. The sample may be reheated and cooled a number of times to obtain better information on the shape and temperature of thermal arrests. In this set of experiments, we have been concentrating on the liquidus part of the phase diagram as we want to determine the maximum-melting composition, which is the one best suited for crystal growth.

Quench-type experiments are being used in conjunction with thermal analysis to aid in the determination of the best composition for growing crystals. In these studies, reactant materials (typically 200 mg) are weighed in the desired proportions, sealed under vacuum in silica-glass containers and heated for lengths of time necessary to obtain equilibrium assemblages for a given temperature. They are then chilled to room temperature by dropping the hot ampoule into a container of ice-water immediately upon removal from the furnace. Phases are identified using standard microscope and x-ray powder diffraction methods.

2.3 Crystal Growth

2.3.1 Basic Overview

Since these compounds melt congruently, crystals can be grown using the Stockbarger technique. Requirements for growing crystals of sulfosalt-type materials include slow growth rates (5-20 mm/day) and steep temperature gradients (5-15°C/mm) at the solid-liquid interface in the crystal-growing furnace.

Portions of polycrystalline reactant material are sealed under about 0.8 atm pressure of pure argon into silica-glass "crystal-growing" tubes which contain a pointed protrusion at the bottom to initiate single crystal growth. The argon pressure in the tube suppresses the presence of vapor during the run.

Cylindrical silica-glass furnaces have been used for much of our crystal growing. Each furnace consists of two heated zones separately controlled by variacs: an upper high-temperature zone and a lower low-temperature zone. The temperature gradient at the solid-liquid interface can be varied by adjusting the voltages to the two windings. As the crystal-growth tubes containing the melts are dropped slowly through the furnace, the melts crystallize when the temperature reaches that of the solidification (melting) point. The grown crystal is allowed to anneal at the temperature of the lower furnace (usually set at about half the melting temperature), and is then cooled to room temperature over a period of two to three days.

Although these furnaces have been used successfully in growing sulfosalt crystals of high quality, they have deficiencies which tend to be more pronounced in effect when we are dealing with materials having steep liquidus curves around the maximum melting composition and/or eutectic interference problems. They are uninsulated and have the temperature "controlled" directly by variacs, which makes crystals growing in them more sensitive to changes in ambient temperature and in line voltages. Both of these problems can affect the interface gradient and its position in the furnace. Some of the adverse results include banding, precipitation of other phases, and the development of polycrystallinity due to breakdown at the solid-liquid interface. These furnaces are useful for survey crystal growth runs and will continue to be used for this purpose.

Studies of crystals of Tl_3VS_4 grown in these systems indicated that these shortcomings were having a deleterious effect on the quality of our crystals. Phase diagram investigations into the system Tl-V-S (discussed in Section 3) tended to confirm this conclusion. As a result, a furnace system was designed to provide a satisfactory environment for high quality growth. This controlled growth furnace is used particularly in connection with our studies of the effects of crystal growth parameters (e.g., growth rate, gradient, rate of cooling) on crystal quality.

2.3.2 Controlled Growth Furnace

The complexities associated with many ternary chalcogenides, including Tl_3VS_4, and their resulting sensitivity to growth conditions, mentioned above, impose a number of requirements on a crystal growth furnace.

1. Both long-term and short-term temperature stability are needed. Temperature fluctuations produce perturbations in growth rate, which can in turn produce compositional inhomogeneities which seriously degrade crystal quality.
2. A steep gradient at the growth interface is desirable in order to provide convective mixing of the melt.
3. Slow and uniform growth rates allow diffusion of impurities away from the solid-liquid interface to improve homogeneity, provided requirement 1 is satisfied.
4. Susceptibility to damage from thermal stress requires that the grown crystal be cooled slowly.
5. In order to evaluate meaningfully the effect of small compositional changes on crystal quality, growth conditions must be closely reproducible from one run to the next.

In an attempt to meet the above requirements, the furnace shown schematically in Fig. 1 was designed and constructed along with a suitable control system. The furnace consists of two independently controlled heaters whose temperatures are adjusted to provide the desired gradient between them. Each heater zone is lined with a massive nickel heat leveler which helps linearize the temperature along that zone, sharpens the gradient between the zones, and provides a large thermal mass to aid in temperature stability. Chromel-alumel control thermocouples are positioned against the heater windings for maximum sensitivity.

The mechanism used to lower the crystal growth ampoule through the gradient consists of a screw and ball nut arrangement which converts the output of the synchronous motor and gear box to a smooth linear drive. The drop rate can be varied over a wide range of fixed gear ratios.

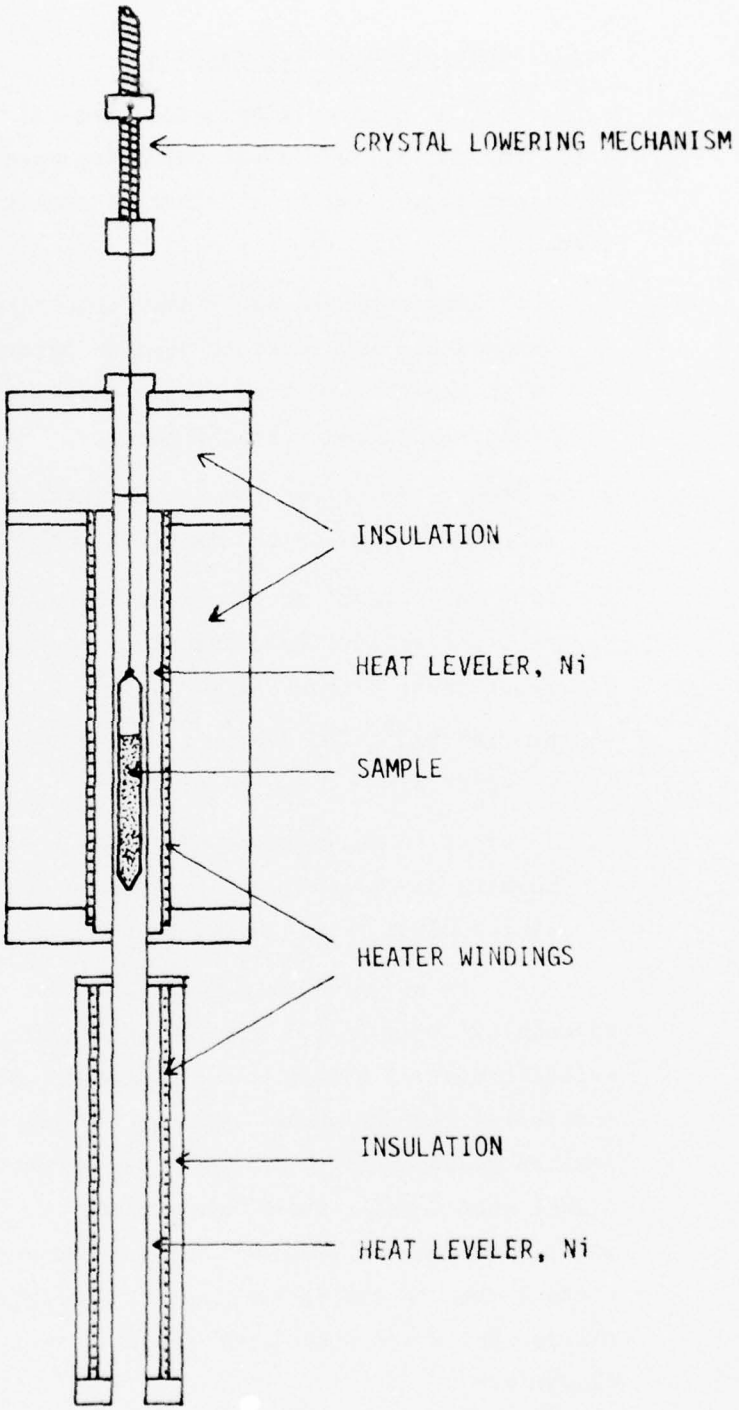

SULFOSALT CRYSTAL GROWING FURNACE

Fig. 1.

Each heater is controlled by an independent system. The control unit for each consists of a L&N model W AZAR recorder with a CAT controller which in turn controls the gate of a Research Inc. Model C32 phaser. Control set point is determined by an external ten turn helipot which can be set manually or driven by a synchronous motor and gear box through a clutch for controlled cooling. Typically, temperature as measured by the control thermocouple output oscillates $\pm$0.05°C about the set point. Temperature fluctuations in the working region of the furnace should be less. This is also a measure of reproducibility of temperature settings from one run to another. The furnace and control system are shown in Fig. 2.

The measured temperature profile in the gradient region of the furnace is shown in Fig. 3. This profile has been used for all the growth runs carried out to date. The gradient at the growth interface is about 100°C per cm. The gradient can be changed by adjusting the heater temperatures and/or the position of the movable lower heater.

A typical crystal growth experiment proceeds as follows. The pre-reacted sample, sealed in a quartz crystal growth ampoule, is suspended in the lower zone of the cold furnace. Both furnace zones are then brought up to temperature. The ampoule is then moved gradually into the upper hot zone such that melting proceeds from the top of the sample. This procedure prevents possible cracking of the ampoule during melting. The ampoule is positioned such that the bottom tip of the sample remains unmelted so as to nucleate growth. When steady state thermal conditions are achieved, the sample is lowered through the gradient at the desired rate. Growth rates used to date have been 0.94 to 4.70 cm per day. When the entire ampoule has passed into the lower zone, the recorder spans and set points are adjusted so that the controlled cooling to room temperature can be carried out without additional adjustment of span or zero suppression. The degree of control is reduced during cooldown but, since the sample is solid, this should

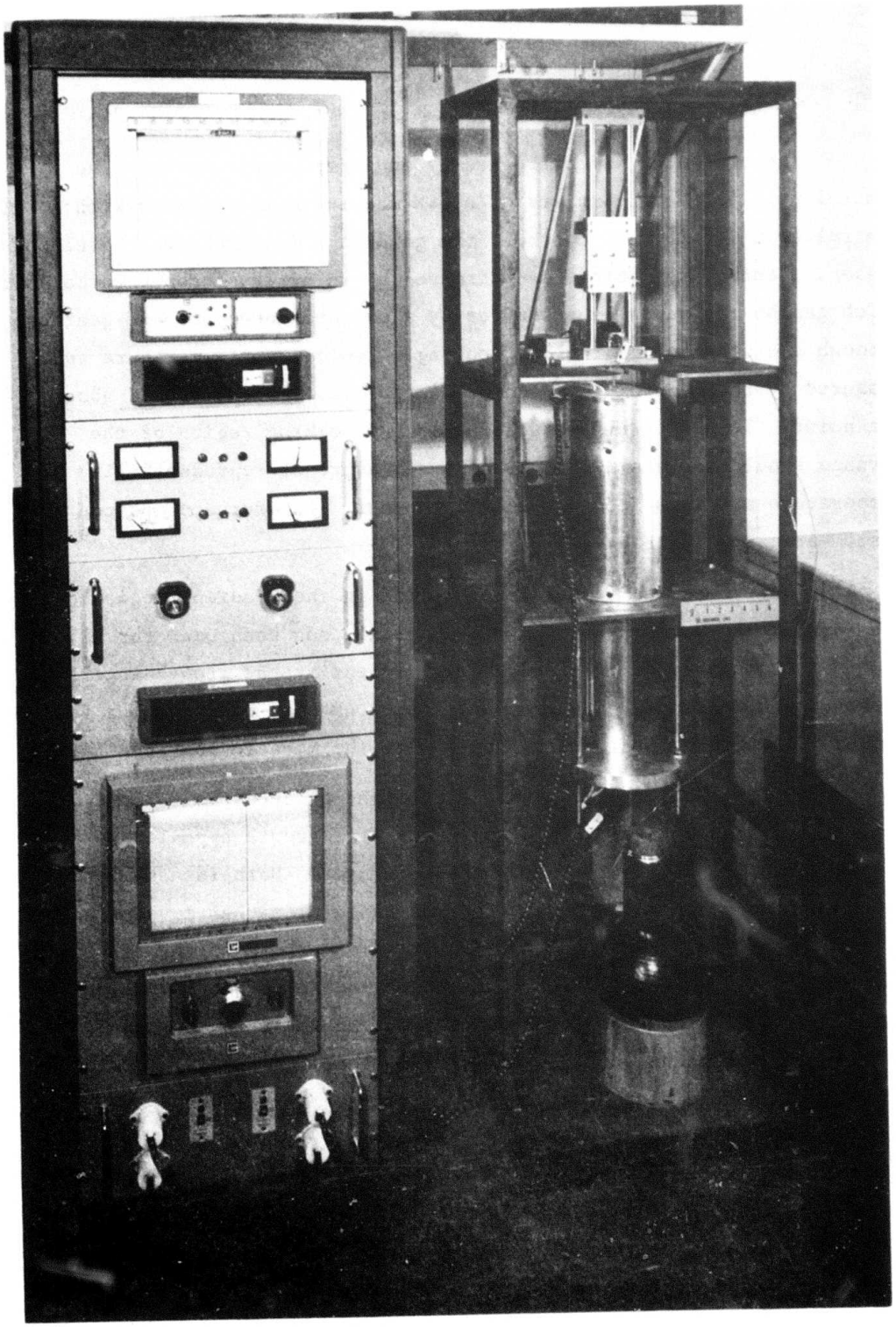

Fig. 2. New semi-automated two-zone furnace and control system.

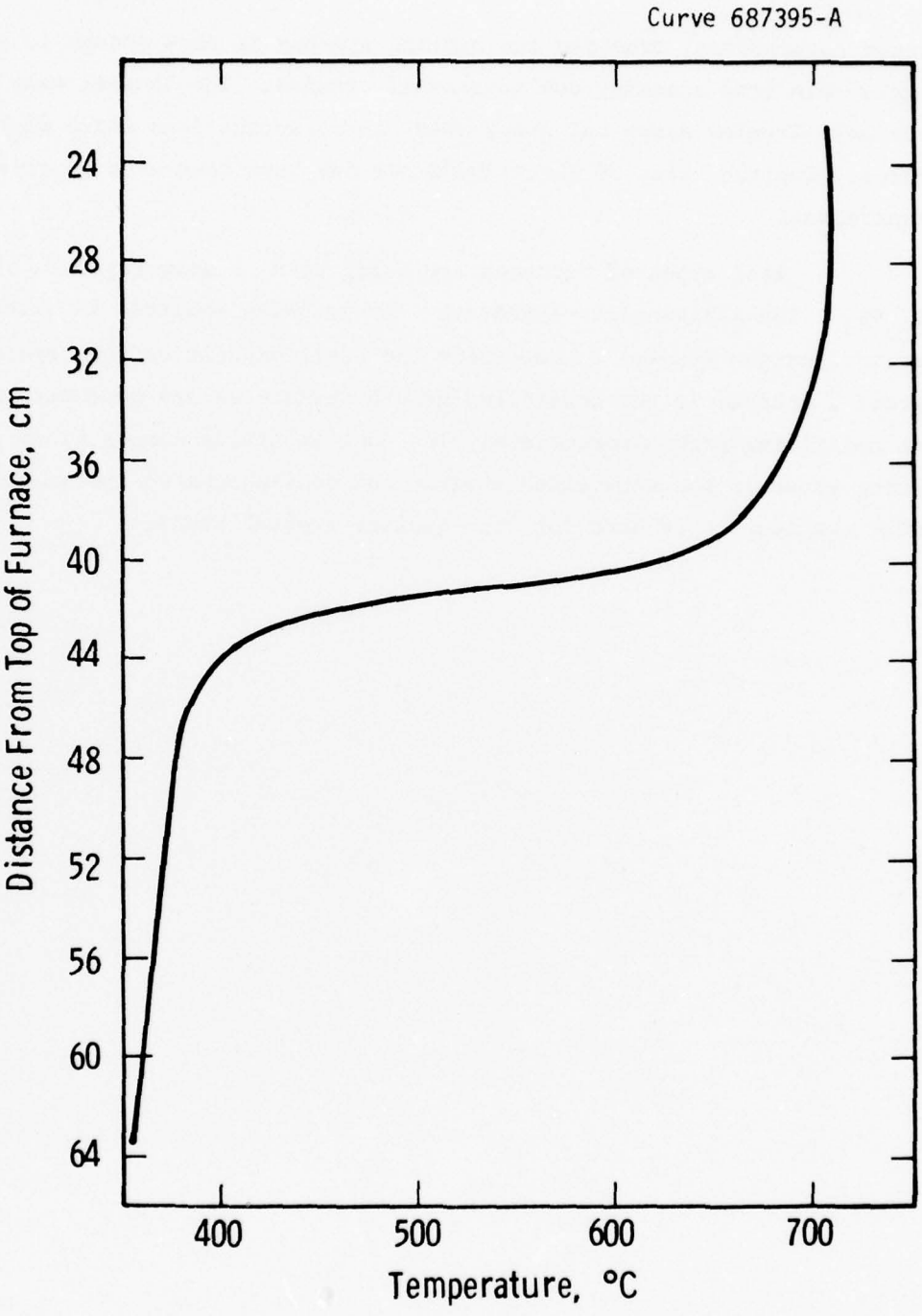

Fig. 3 — Temperature profile of crystal growth furnace

cause no problems, provided the cooling process is slow enough to prevent the sample from cracking due to thermal strains. The thermal mass of the heat leveler damps out minor short term fluctuations which might occur. Cooling rates of about 100°C per day have been used in recent experiments.

Both types of furnaces are being used to grow crystals of Tl_3VS_4. The silica-glass furnace set-up is being employed in directional solidification studies to determine the best composition for crystal growth, whereas in the controlled growth furnace we are concentrating on optimizing growth parameters. The most promising compositions are being grown in the controlled environment semi-automated system and will continue to be used for high quality crystal studies.

3. PHASE EQUILIBRIA AND CRYSTAL GROWTH STUDIES

3.1 Compounds in the System Tl-V-S

The composition of compounds in the system Tl-V-S can be described in terms of a phase diagram (Fig. 4) on which the compositions of many known binary and ternary compounds are plotted. There are four phases along the binary Tl-S, and a large number reported along the binary V-S, of which six are shown on the diagram. It must be noted that the existence of a compound of composition V_2S_5 is uncertain.[1] The V-S binary has compounds with large ranges of nonstoichiometric compositions, and the compositions given here are approximations. There is only one confirmed ternary compound, Tl_3VS_4.

3.2 Study of Melting Relations

In studies of phase relations in ternary systems, it is often found that ternary compounds lie on or near composition joins connecting two compounds in two of the binary systems. When all the equilibrium tie lines lie in the plane of the join, then the join may be treated as pseudobinary, i.e., a two-component system. Even if the join is not a true pseudobinary, it is convenient to use it as a basis of gathering data on phase relationships near the compound of interest. Our approach to the problem of determining the best composition for growth of reproducible high-quality crystals of Tl_3VS_4 was by first studying phase relations along one such join to determine the maximum melting composition, location of eutectics, solid solution, and possible secondary solid phases, particularly near this composition. We realized that the best composition was probably ternary and therefore would not lie on a join. But the information derived from this study would give us a starting point for exploration into ternary relations around the maximum melting

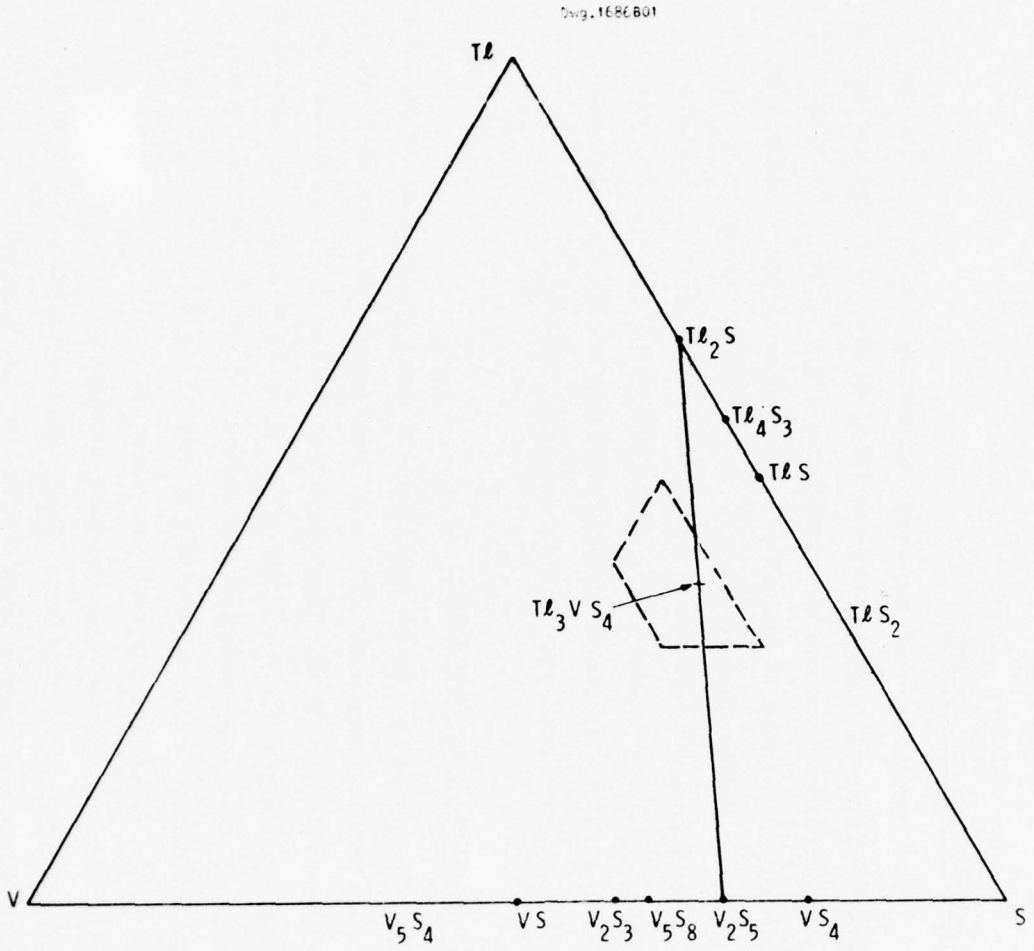

Fig. 4 — The system Tℓ - V - S showing compounds and possible pseudo binary joins through the ternary compound $Tℓ_3VS_4$

composition. We selected the join Tl_2S-V_2S_5 for our initial investigation, based upon earlier work on other sulfosalt systems.[2,3]

A number of thermal analysis runs were made using selected compositions along this join (Table 1). Unfortunately, reproducibility of freezing (melting) point temperatures was poor, particularly where compositions deviated by more than a few percentage points from the stoichiometric composition. There was considerable supercooling (as much as 100°C in a few instances), and there were additional arrests indicating the presence of other ternary phases, and/or possibly of ternary eutectics. For example, samples of composition $Tl_{1.6}V_{0.4}S_{1.8}$ showed arrests corresponding to four transitions (see Fig. 5). The highest temperature transition, corresponding to the liquidus surface, was unclear on cooling curves, but could be identified on heating curves as the termination of melting. This temperature ranged from 500°C to 505°C. The next arrest, the sharpest, occurred at 430 to 437°C. Two lower arrests were in the vicinity of 255 and 235°C. Other compositions along the Tl_2S-V_2S_5 join gave thermal arrests which were clearly associated with the same transitions but at somewhat different average temperatures. Poor reproducibility can arise from several causes. In most cases more than one is operational. When supercooling is severe, the heat evolved may be insufficient to bring the temperature of the sample up to the true value of the transition temperature. This behavior was quite apparent on cooling curve arrests corresponding to the liquidus for many compositions leading to low values for liquidus temperatures. In some cases a better value could be derived from the heating curve. Sluggish kinetics can produce similar results. The magnitude of the error introduced can be strongly dependent on sample composition. Eutectic valleys can further complicate the interpretation of arrests in ternary systems.

A partial cooling curve for Tl_3VS_4 is shown in Fig. 6. Note the degree of supercooling and the low temperature arrest. The latter is strong evidence that the stoichiometric composition is not maximum melting.

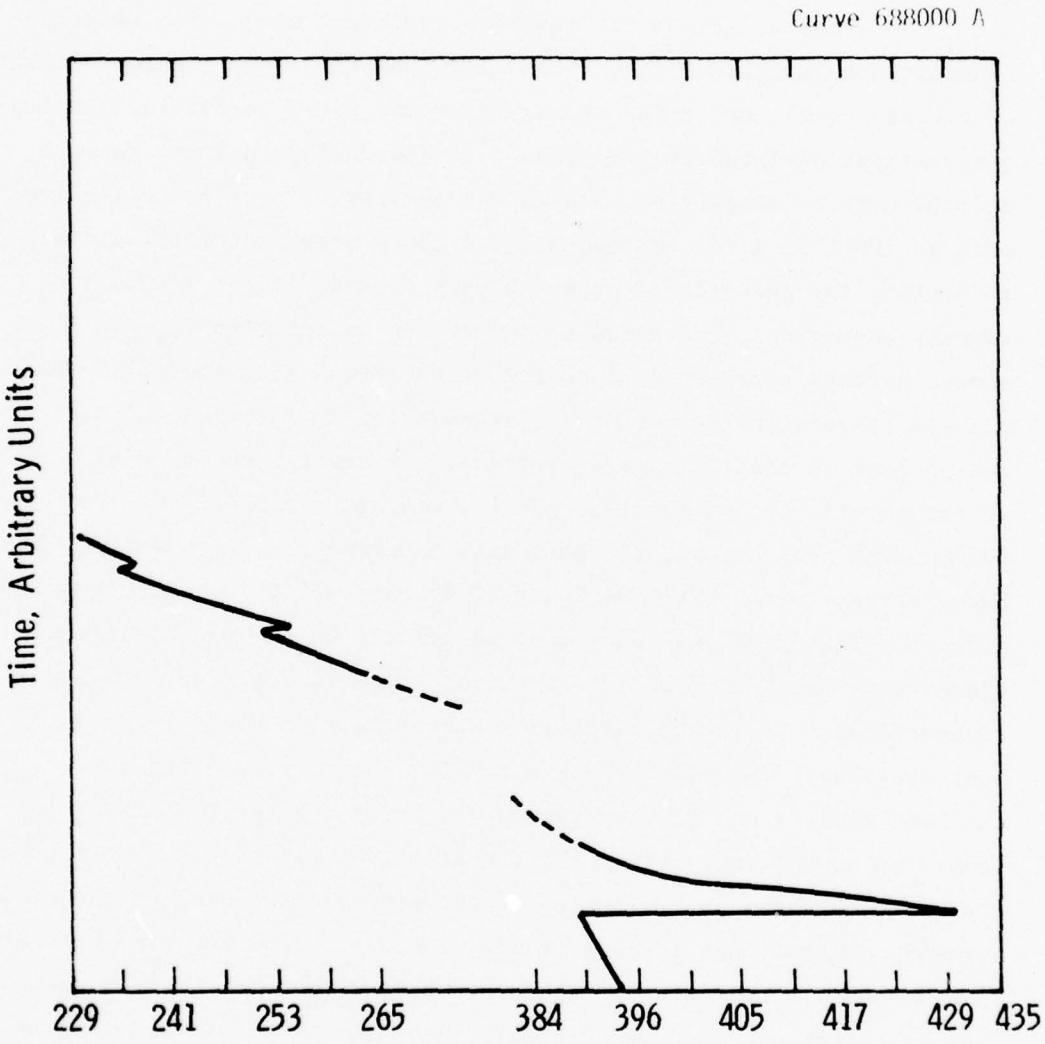

Fig. 5 – Portion of cooling curve for $Tl_{1.6}V_{.4}S_{1.8}$

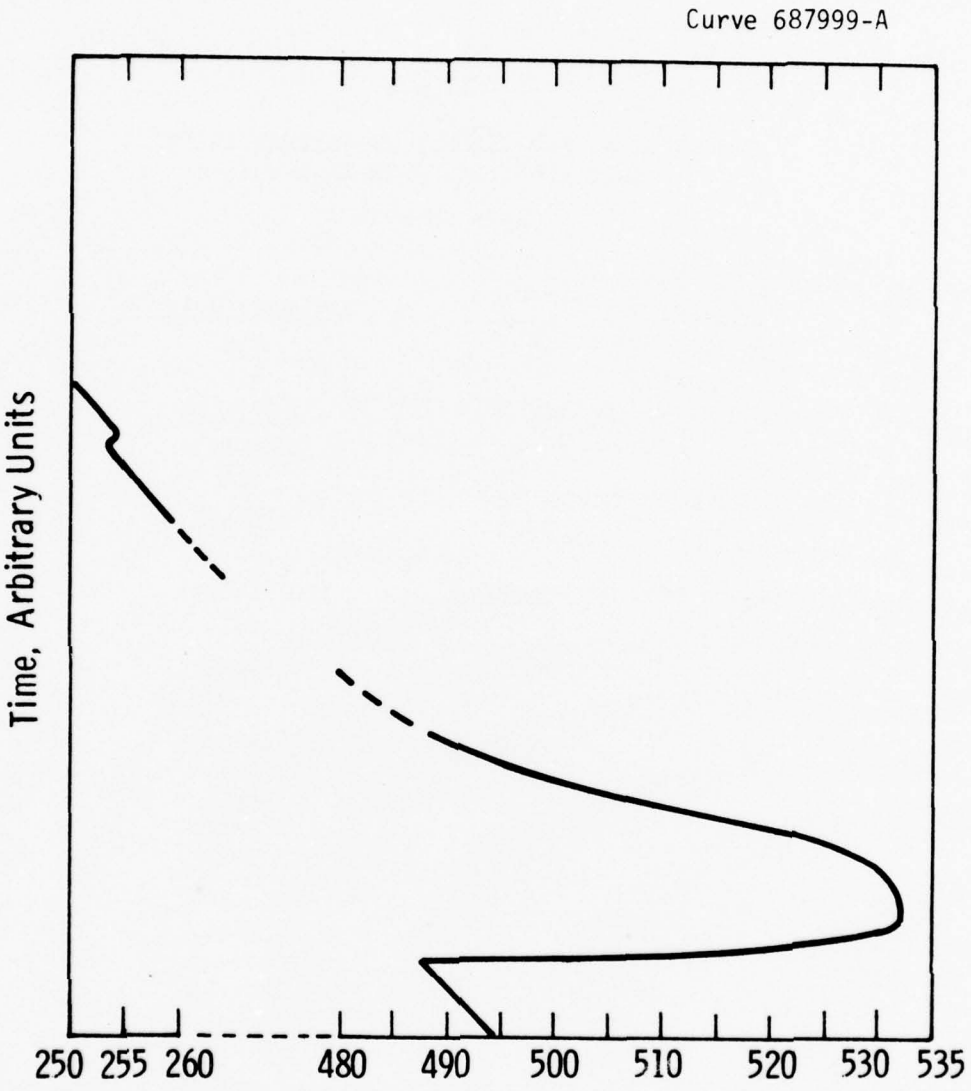

Fig. 6 — Portion of cooling curve for $T\ell_3$ V S_4

Table 1

COMPOSITIONS AND ARRESTS OF THERMAL ANALYSIS RUNS ALONG THE JOIN Tl_2S-V_2S_5

Given in mole %

Tl_2S	V_2S_5	*Arrests, T in °C
95	5	432 411
90	10	444-446 419-422 414
87.5	12.5	420-420.5 402
86.25	13.75	418.5-421 391
85	15	419-423 411.5-413.5
82.5	17.5	506.5-514 450.5-456 444 423-424 253
80	20	500-505 430-437 254.5-255 233-236
77	23	522-527
76	24	521-533 407.5-409
75.25	24.75	524-534 408-409
75	25	522-533 259
74	26	530-532

Table 1 (con't)

Tl_2S	V_2S_5	*Arrests, T in °C
†70	30	480.5-490
†65	35	434.5-445.5 418-424 358-367

*In the case of arrests corresponding to the liquidus, the observed extreme supercooling would cause the numbers derived from the cooling curve to be low. The range of temperatures given here are taken from both heating and cooling curves.

†The upper temperatures given here are not those of the highest melting homogeneous melt of these compositions. There was a high-melting temperature compound which remained solid throughout the runs, so that complete melting did not occur.

From the thermal analysis we were able to determine that there was an eutectic at a temperature of about 420°C occurring at the approximate composition 88 Tl_2S-12 V_2S_5. The overwhelming majority of the runs were made on the Tl_2S side of the join, as there was incomplete reaction with the formation of a very high melting point compound (or compounds) only a couple of percentage points away from the stoichiometric composition on the V_2S_5 side. We therefore concentrated on a small portion of the join near the stoichiometric composition. We also performed a series of quench-type experiments at selected compositions and temperatures (Table 2) along this join, and were able to determine the relative amounts of extraneous phases present at the various compositions. Here too, we concentrated on compositions on the Tl_2S-rich side of Tl_3VS_4.

Results of these runs were examined microscopically in polished sections under reflected light. Significant amounts of second and even third phases were present in all but two compositions, 75 Tl_2S-25 V_2S_5 and 75.25 Tl_2S-24.75 V_2S_5, with the latter showing the fewest impurities. Polished sections of runs at the three higher temperatures of composition 88 Tl_2S:12 V_2S_5 showed two phases with eutectic appearance. At lower temperatures, there was no pattern to the intermixing. Those of composition 80 Tl_2S:20 V_2S_5 contained two phases, with one greater than the other. There was no pattern to the intermixing. At composition 78 Tl_2S:22 V_2S_5, three phases were discerned, one of which comprised less than 5% of the area and showed lath-like morphology. The other two phases showed no pattern to their intermixing, but one was in excess of the other (approximate ratio 7:3). At the stoichiometric composition, two phases were observed which varied in ratio depending upon the temperature. At the higher temperatures, the polished section showed less than 2% second phase. Only one run was made at composition 75.25 Tl_2S: 24.75 V_2S_5, and it too showed some second phase which comprised approximately 1% of the area. Sections of runs on the V_2S_5-rich side (composition 72 Tl_2S:28 V_2S_5) were polyphase and often rather blotchy-looking. Pitting was observed in most of the polished sections, and

Table 2

COMPOSITIONS AND TEMPERATURES USED IN QUENCH-TYPE EXPERIMENTS ALONG THE JOIN Tl_2S-V_2S_5

Tl_2S (mole %)	V_2S_5 (mole %)	T, °C
95	5	552
88	12	240
		402
		508
		530
		552
80	20	240
		402
		508
		530
78	22	240
		402
		530
		552
75.25	24.75	552
75	25	240
		402
		508
		530
		552
72	28	240
		402
		508
		530
		552

was at its worst at the last mentioned composition. The least amount of pitting was found at compositions 75.25 Tl_2S:24.75 V_2S_5 and 75 Tl_2S:25 V_2S_5. These results indicate that the composition which we need does not lie on the Tl_2S-V_2S_5 join, but rather is ternary, although close to this join.

By using data from thermal analysis and quench-type experiments, we found that there was a maximum melting composition (approximately 75.25 Tl_2S-24.75 V_2S_5) along this join. Figure 7 shows the liquidus of this small portion of the join. Because of the difficulties encountered in attempting to work out phase relations along this join, we came to the conclusion that it was not pseudobinary, and therefore abandoned further efforts in this area.

We then proceeded to perform a series of crystal growth experiments using the above-mentioned maximum melting composition as a starting point, and varying the compositions of the reactant mixtures by small increments around it. While we have not as yet determined the best composition, we have noticeably improved the quality of our crystals by growing them off-composition on the Tl-S rich side of the stoichiometric composition.

After examining results of some of our crystal growth runs, we decided to look into phase equilibria relations near the Tl_3VS_4 composition on two other joins, TlS-VS and S-"Tl_3VS_3" to search for possible eutectics which might interfere with the growth of high quality crystals, and also perhaps to enable us to "map" melting points to determine the ternary maximum melting composition. We have thus far performed only a few experiments along the TlS-VS join, but there is evidence of a eutectic within 3 or 4 mole percent on the TlS-rich side. Once again, the problem of incomplete reaction occurred on the VS-rich side within 2-1/2 mole percent excess VS. There was also supercooling, although not very severe. We are continuing to study melting relations within a narrow range along this join.

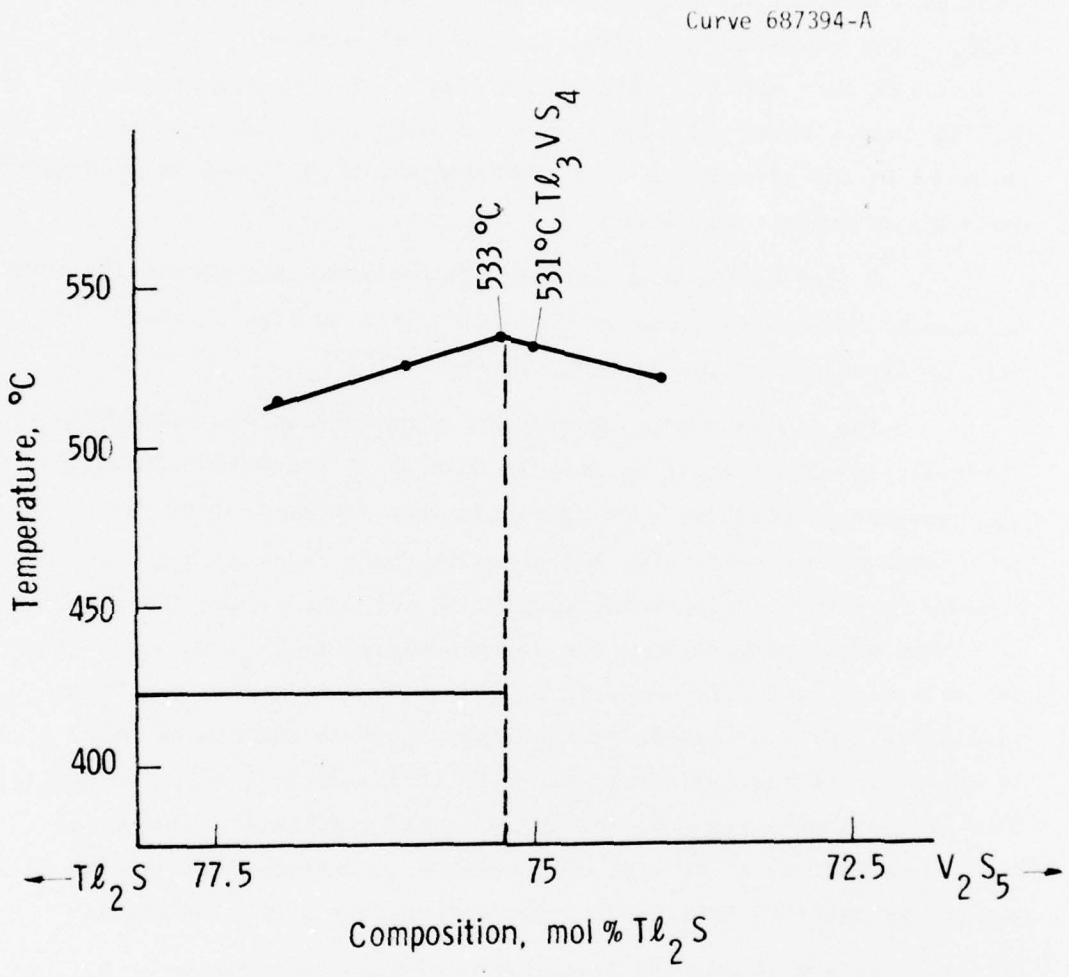

Fig. 7 — Portion along "pseudo binary" join $T\ell_2 S - V_2 S_5$ around the composition $T\ell_3 V S_4$ showing approximate liquidus curve

We also have been investigating a small portion of the join S-Tl_3VS_3. While we have only run a few experiments, there are indications of a maximum melting composition on the sulphur rich side of Tl_3VS_4. The compound Tl_3VS_3 is hypothetical because we have not been able to prepare pure phases of this composition by cooling from a melt. If such a compound exists (it has not been reported in the literature to our knowledge), then it may be incongruently melting, or may not be stable.

A plot of the compositions examined thus far within the area defined by the dashed lines on Fig. 4 is given in Fig. 8, where this area is expanded for the sake of clarity.

The Tl-V-S system appears to be quite complex, making it difficult to obtain phase equilibria data using standard techniques. The experiments which we have performed thus far on several joins show much supercooling and often multiple arrests, and reproducibility of data, especially where the composition deviates by more than a few percent from the stoichiometric Tl_3VS_5, is poor. There are eutectics near this composition, but they have not as yet been identified. Crystal growth studies indicate that the single phase field is extremely narrow, and that there is little, if any, solid solubility. This last statement is corroborated by x-ray diffraction studies of lattice parameters at several compositions. These conditions make it imperative that the best composition for crystal growth be found.

We are conducting optimization studies predominantly by directional solidification runs on samples having incremental differences in composition. Additional thermal analysis and quench-type experiments also are being performed where necessary, but the greater part of the compositional refinement will be done by crystal growth studies.

We have grown crystals of improved quality from near non-stoichiometric compositions, but reproducibility still is not good. We have yet to obtain crystals free from defects.

Fig. 8 — Expanded section of the ternary system Tℓ - V - S in the region of the composition $Tℓ_3VS_4$, showing some of the phase equilbra runs

Despite the problems encountered, the quality of the crystals that we have been growing recently has improved to the extent that impurities have become difficult to see using ordinary reflected light microscopy. We therefore examined a portion of one of our more recent crystals under the infrared microscope to determine the usefulness of this technique as an aid in evaluating crystal quality. The crystal was generally of good quality, but some small inclusions were clearly visible within the slice. This instrument will be used in future runs as a standard evaluation technique.

3.3 Study of Crystal Growth Parameters

We have been conducting experiments in our semi-automated two-zone furnace and control system on the effects of growth parameters on crystal quality. The first set of experiments, presently being conducted, is concerned with rate of growth at constant composition. Three rates initially are being used, 0.94, 1.9 and 4.7 cm/day. The boule grown at the fastest rate was not a single crystal, but instead consisted of five or six intergrown crystals. Cracking in the crystals was not observed, however, The crystal grown at the intermediate speed was single, but had several cracks in it. Examination of a polished section under the microscope showed only a very small amount of widely disseminated fine particles of second phase. We are growing another crystal at this speed as there were external problems during the first run which may have caused the cracking.

4. STUDIES OF ACOUSTIC SURFACE WAVE PROPERTIES

4.1 Overall Objectives

The acoustic work comprises two areas of study. The first involves the measurement of material constants such as the elastic, piezoelectric, dielectric constants, the density, and the temperature dependence of these constants. These numbers are then used to calculate surface wave velocities in various cuts and propagation directions as a function of temperature. Orientations are considered useful when the temperature coefficient and power flow angle are small and the effective surface electro-mechanical coupling factor is large.

The second area of study involves SAW device fabrication and testing on the sulfosalt materials. This work is concerned with techniques of cutting, polishing, and photolithography, and in general the surface quality of a finished crystal device.

4.2 Determination of Material Constants

The measurements of the material constants are proceeding in stages. The earliest work involved measurement of the bulk wave velocities,[4] the density,[4] the thermal expansion coefficient,[5] and the first order temperature coefficients[5] of the elastic constants. These numbers combined with an approximate dielectric constant value[5] then were used to calculate surface wave velocities, power flow angles, surface wave coupling efficiencies, and temperature coefficients of delay for various cuts and propagation directions. Some temperature-stable directions were found and were verified experimentally.[5] The agreement between theoretical and experimental temperature-stable directions was not impressive, and it was decided to measure the dielectric and

piezoelctric constants more accurately, and to measure their temperature dependence. We are currently performing these measurements.

The dielectric constant was determined by measuring the capacity of a capacitor filled with Tl_3VS_4. The area of the plates and the thickness between plates was accurately known. Vapor-deposited Cr-Au films were used for the plates, and were deposited on either (100) faces or (110) faces. The (100) face configuration gave the clamped capacity directly whereas the (110) face measurements needed to be corrected[6] for the piezoelectric strain caused by the electric field. Most of the measurements were done on samples no thicker than 0.1 cm at 20 KHz using Boonton capacity bridge.

Once the dielectric constant was known, the piezoelectric constant could be redetermined from the value of measured bulk shear wave velocities. The bulk shear velocity for propagation down the [100] is independent of the shear wave polarization and depends on the square root of the elastic constant c_{44}. The bulk shear velocity for propagation down the [110] with polarization along the [001] depends on $(c_{44} + e^2/\varepsilon)^{1/2}$ where e is the piezoelectric constant and ε is the dielectric constant. Measurement of the above two velocities and ε allows one to calculate e according to the formula

$$e^2 = \varepsilon\rho(V^2_{[110],[001]} - V^2_{[001]}) \qquad (1)$$

where ρ is the density and V is the appropriate shear wave velocity. All of the measured constants mentioned thus far appear in Table 3.

The temperature coefficient of the dielectric constant was obtained by performing the capacity measurements mentioned above as a function of crystal temperature. For an orientation where the electric field does not cause piezoelectric strain, the capacity C is

$$C = \frac{\varepsilon A}{\ell} \qquad (2)$$

and

$$\frac{1}{C}\frac{\partial C}{\partial T} = \frac{1}{\varepsilon}\frac{\partial \varepsilon}{\partial T} + \frac{1}{\ell}\frac{\partial \ell}{\partial T} \qquad (3)$$

where A is the cross-sectional area of the capacitor plates, ℓ is the separation between plates, and T is the temperature. The thermal expansion coefficient $\frac{1}{\ell}\frac{\partial \ell}{\partial T}$ was measured separately using a dilatometer technique. By combining the dielectric constant temperature coefficient with the temperature coefficient of c_{44} and of the stiffened c'_{44}, the temperature coefficient of the piezoelectric constant can be calculated. Our initial measurements of the temperature coefficient of the stiffened c'_{44} contain some scatter, which may be due to microscopic cracks in the samples used. Consequently, there is currently some uncertainty as to the value of $\frac{1}{e}\frac{\partial e}{\partial T}$. All of the first order temperature coefficients measured so far also appear in Table 3.

We expect that the next set of measurements of the crystal constants will be performed on crystals of higher quality, and will therefore have greater accuracy. As the crystal quality improves, we will also continue work on the determination of acoustic attenuation. The attenuation measurements consist of initiating a pulse (compressional or shear) in a Tl_3VS_4 bulk wave delay line and observing the echo decay on an oscilloscope screen. To insure proper interpretation of the echo train, we superimpose an exponential[7] trace on the echo pattern to verify that the decay we observe is exponential. We check these results by measuring the bulk attenuation using a c.w. standing wave technique.[8] These two techniques yield attenuation coefficients which agree to within 10%. For samples examined over the last half year, the attenuation constant for compressional waves propagating down the [100] in Tl_3VS_4 is 0.3 dB/μs at 30 MHz; for shear waves propagating down the [110] polarized along the [001], it is 0.9 dB/μs at 30 MHz.

4.3 Surface Wave Properties

The constants appearing in Table 3 can now be used in calculating surface wave properties. We have determined velocities, coupling

Dwg. 1684845

TABLE 3 CONSTANTS OF Tl_3VS_4 AT ROOM TEMPERATURE

Elastic Constants	C_{11}	4.85×10^{10} N/m^2
	C_{12}	1.65
	C_{44}	0.47
Piezoelectric Constant	e_{14}	0.50 c/m^2
Relative Dielectric Constant	$\varepsilon_{11}/\varepsilon_0$	29.0
Density	ρ	6.14×10^3 kg/m^3
First Order Elastic Temp. Coeff.	$\frac{1}{C_{11}} \frac{\partial C_{11}}{\partial T}$	-5.72×10^{-4}/°C
	$\frac{1}{C_{12}} \frac{\partial C_{12}}{\partial T}$	-2.10
	$\frac{1}{C_{44}} \frac{\partial C_{44}}{\partial T}$	0.98
First Order Piezoelectric Temp. Coeff.	$\frac{1}{e_{14}} \frac{\partial e_{14}}{\partial T}$	$\simeq -3.2 \times 10^{-4}$/°C
First Order Dielectric Temp. Coeff.	$\frac{1}{\varepsilon_{11}} \frac{\partial \varepsilon_{11}}{\partial T}$	-0.25×10^{-4}/°C
Thermal Expansion Coeff.	$\frac{1}{\ell} \frac{\partial \ell}{\partial T}$	0.25×10^{-4}/°C

efficiencies, power flow angles, and temperature coefficients of delay for surface waves propagating on the (001), $(1\bar{1}0)$, and (111) planes of Tl_3VS_4. We show only the results for the (001) plane in Fig. 9. The theoretical work on the $(1\bar{1}0)$ and (111) planes is not as yet completed, but some information concerning surface wave properties for propagation on these planes can be found in Ref. 4. Although the experimental points do not appear in Fig. 1, we have measured the velocity, the effective surface coupling constant, and the temperature coefficient of delay for surface waves propagating down the [110]. The agreement between experiment and theory is excellent.

Figure 9 graphically portrays the features which make Tl_3VS_4 attractive for device applications. The surface wave velocity is about three times smaller than for quartz; therefore, SAW devices using Tl_3VS_4 can be made three times smaller than those using quartz. The coupling efficiency for SAW propagation along the [110] is at least ten times that of quartz and the power flow angle is zero. For this propagation direction in the (001) plane the temperature coefficient is not zero but is small ($\sim$20 ppm/°C).

We expect to have more information about other cuts and propagation directions after we have made necessary alterations in the computer program used in the calculation of surface wave properties. We are investigating the behavior of the computer programs under the conditions that prevail when it does not produce meaningful results. It has been observed that solutions are obtainable in the difficult regions provided a good initial guess is made at the velocity of the wave. The root finding subroutine is evidently failing so we have replaced it with another one that we believe will give better results. A test of the new program is underway. We anticipate the need to extend the program so that it will allow for pseudo-surface waves, that is, those that are coupled with the bulk waves so that the amplitude decays in the direction of propagation.

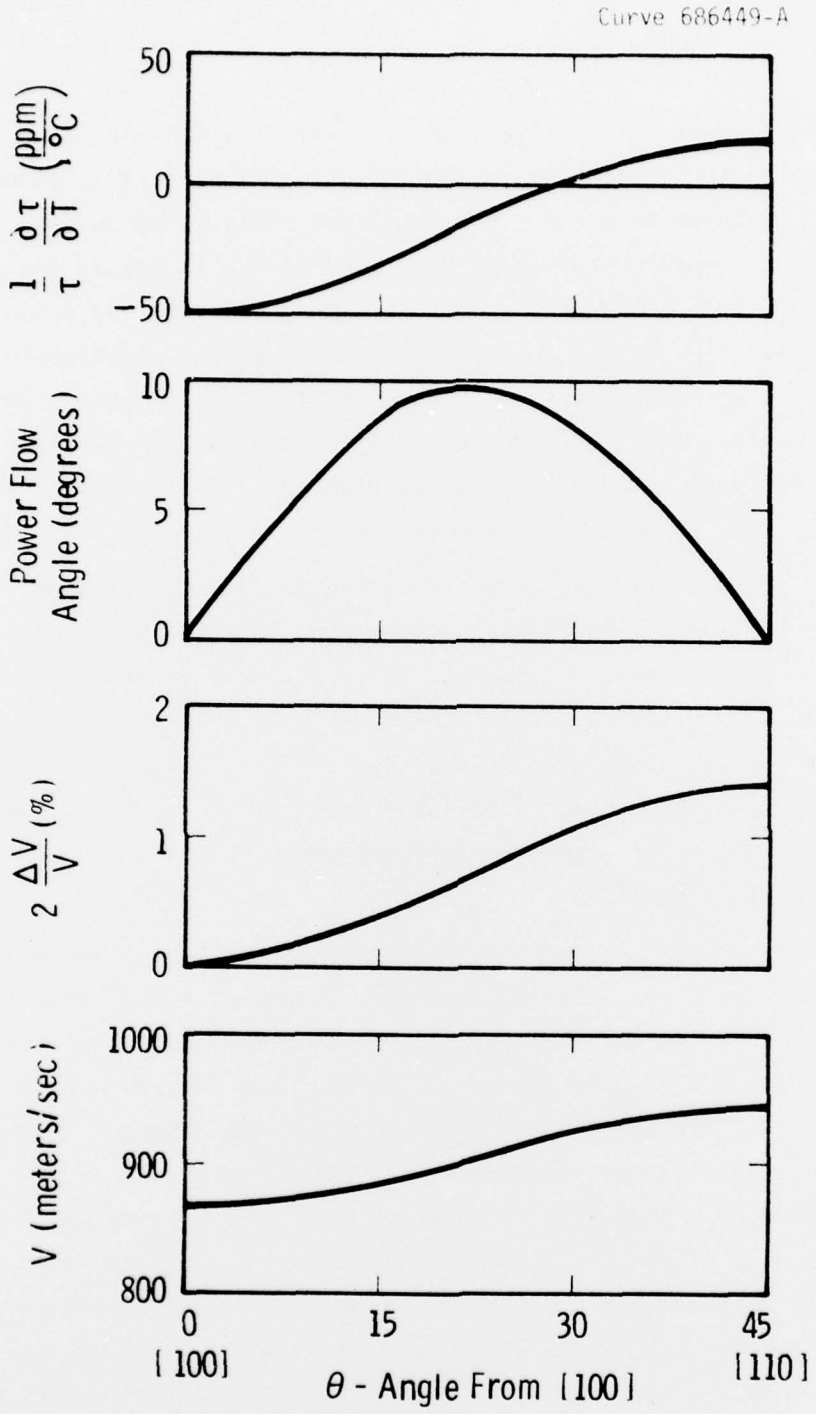

Fig. 9 – Surface wave velocity, $2\frac{\Delta V}{V}$, power flow angle, and temp. coeff. of delay for propagation on the (001) plane of Tl_3VS_4

4.4 Device Fabrication

Tl_3VS_4 presents some problems in fabrication of surface wave devices. The material is soft (Mhos hardness of about 2.5) and care must be exercised in the cutting and polishing of the crystal. We have recently been able to get fairly good surfaces on samples as thin as 10 mils. This was accomplished by first cutting slices about a millimeter thick with a beryllium-copper wire loaded with 45 micron diamond, and then polishing with a polishing compound on a rotating lap. The crystals that are of high quality hold together and withstand rough handling much better than the poor quality crystals. There is, therefore, good reason to expect that in the near future a high percentage of crystals will be easy to handle.

Using a photolithographic technique, a SAW filter was fabricated on the 001 face of Tl_3VS_4 for SAW propagation along the [110]. The crystals used for this fabrication study were not of the highest quality, but did allow us to develop fabrication techniques suitable for this material. A SAW filter was fabricated and tested and is discussed fully in Ref. 9. The most serious problem with the filter is the high insertion loss. This was not expected because of the high coupling efficiency of this material. It was this high insertion loss which lead us to examine the surface layer of the crystal more closely.

4.5 Study of Surface Damage Caused by Cutting and Polishing

The nature and extent of the damage layer remaining on (100) oriented Tl_3VS_4 crystals after cutting and polishing has been investigated using x-ray and electron diffraction methods. Since a chemical etch suitable for removing surface layers has not been developed, etching was performed using a Veeco ion beam milling system. With a milling current of .8 mA/cm^2, anode voltage of 1 kV and bell jar pressure (with argon) of 2×10^{-4} Torr, material was removed from the crystal surface at a rate of $\sim$8-9 μ/hr.

Visual evidence of mechanical damage was still present after 12μ had been removed. Most scratch traces disappeared after the removal of about 24μ. The original polished and the milled surfaces were examined by x-ray and electron diffraction. Evidence based on Weissenberg and Laue diffraction patterns indicated that an amorphous region several microns thick had been induced by polishing. The precise thickness has not yet been established, but appears to lie between 12 and 24μ. In the case of one crystal, after removal of 24μ electron diffraction yielded sharp single-crystal spot patterns showing no trace of amorphous material.

Further ion beam milling studies are being continued to establish the precise depth of damage with the aim of correlating this information with surface wave acoustic measurements being made on the crystals.

Only bulk acoustic attenuation measurements have thus far been made on crystals of Tl_3VS_4. Surface wave values will be determined when we have improved the quality of the crystal surfaces. With imperfect surfaces, scattering and deflection of the surface acoustic wave occurs, which increases the attenuation.

ACKNOWLEDGMENTS

We wish to thank Dr. M. Francombe for studies of surface damage, and W. E. Gaida and S. J. Pieseski for technical assistance.

REFERENCES

1. Gmelins, Handbuch der anorganischen chemie, Vanadium, System No. 48, B1, p. 277. Verlag Chemie, GMBH, Weinheim/Bergstr (1967).

2. G. W. Roland, J. P. McHugh, and J. D. Feichtner, Jour. Electronic Mat. 3, 829 (1974).

3. G. W. Roland, J. D. Feichtner, M. Rubenstein, and W. E. Kramer, Final Technical Report for ARPA Contract F33615-72-C-1976, AFML-TR-76-173 (1975).

4. T. J. Isaacs, M. Gottlieb, M. R. Daniel, and J. D. Feichtner, J. Elect. Mat. 4, 1, 67 (1975).

5. R. W. Weinert and T. J. Isaacs, Proc. 29th Annual Symposium on Frequency Control (1975).

6. T. F. Heuter and R. H. Bolt, "Sonics," New York, Wiley, 1955, Chapter 4.

7. J. de Klerk, Ultrasonics 2, 137-147 (1964).

8. D. I. Bolef and J. de Klerk, IEEE Trans. Ultrasonics Eng. UE-10, 19-26 (1963).

9. R. W. Weinert, T. J. Isaacs, F. Halgas, J. T. Godfrey, and R. A. Moore, 1976 Ultrasonics Symposium Proceedings, IEEE Cat. #76 CH1120-5SU.

MISSION
of
Rome Air Development Center

RADC plans and conducts research, exploratory and advanced development programs in command, control, and communications (C^3) activities, and in the C^3 areas of information sciences and intelligence. The principal technical mission areas are communications, electromagnetic guidance and control, surveillance of ground and aerospace objects, intelligence data collection and handling, information system technology, ionospheric propagation, solid state sciences, microwave physics and electronic reliability, maintainability and compatibility.

Printed by
United States Air Force
Hanscom AFB, Mass. 01731